# Ultrashallow Si $p^+$–$n$ junction fabrication by low energy $Ga^+$ focused ion beam implantation

A. J. Steckl, H. C. Mogul, and S. M. Mogren
*Nanoelectronics Laboratory, University of Cincinnati, Cincinnati, Ohio 45221-0030*

(Received 29 May 1990; accepted 3 August 1990)

The fabrication of ultrashallow Si $p^+$–$n$ junctions by low energy $Ga^+$ focused ion beam implantation has been investigated at energies ranging from 5 to 15 keV. Post-implantation rapid thermal annealing was performed at 600 °C for 30 s to activate the implanted Ga and to regrow the implanted layer. Secondary ion mass spectroscopy (SIMS), spreading resistance profile (SRP), and cross-sectional transmission electron microscopy (TEM) have been employed to characterize the resulting Ga atomic concentration depth profile and the structure of the implanted layer. For 5 keV $Ga^+$ implantation, the cross-sectional TEM (xTEM) measurement yielded an amorphous layer thickness of 9 nm and a line of end-of-range defects 16 nm below the surface [after rapid thermal annealing (RTA)]. The SIMS profiles indicate that only minor Ga channeling occurred during implantation. The SRP measurements give a junction depth of only 20 nm for the 5-keV Ga implants. Leakage current density of 20 $nA/cm^2$ has been measured at 5 V reverse bias.

## I. INTRODUCTION

The inexorable drive towards semiconductor devices with features of smaller dimensions is taking place not only in the horizontal plane, but in the vertical direction as well. One example is the thickness of the gate oxide in metal–oxide–semiconductor field effect transmissions (MOSFETs) which is constantly being reduced. Another example, with which this paper deals, is the *p-n* junction depth of source and drain regions. It is expected that 0.25 $\mu$m complementary metal–oxide–semiconductor (CMOS) technology will require $p^+$–$n$ junction depths of less than 75 nm. It is important to bear in mind that, in addition to junction depth, other important criteria for *p–n* junction performance include a low leakage current and low sheet resistance. To meet these criteria, a number of fabrication approaches have been pursued. They include the implantation of $BF_2^+$, $B^+$, and $Ga^+$ ions at medium to low energy in conjunction with substrate pre-amorphization by Si, Ge, or Ga ion implantation.[1-5] In general, the substrate pre-amorphization greatly reduces ion channeling in the subsequent dopant implantation, but at the price of increased leakage current due to unannealed defects. An alternative approach being pursued is to employ diffusion from a doped poly-Si or silicide layer into a crystalline substrate.[6,7] While low leakage current can be obtained with this technique, the diffusion process is not as controllable as the ion implantation process.[8]

While most *p–n* junction fabrication uses conventional broad-beam implantation systems, focused ion beam implantation has the advantage of localized processing which can tailor the implant conditions for the particular device (albeit at a lower throughput). FIB systems are also more flexible in that the acceleration energy can more easily be reduced than in a conventional implanter. Shallow *p–n* junction fabrication using 25–75 keV FIB Ga implantation has been recently reported.[9] Ga is a heavy *p*-type dopant in Si which has a shallow implantation range and low amorphization dose. During typical Ga $p^+$ implantations, the amorphization of the Si surface layer occurs at only 10%–15% of the total implanted dose. Hence, channeling is predominantly suppressed. Therefore, Ga dopant implantation can be performed without preamorphization, thus substantially reducing the leakage current of the diode.[10] This approach of dopant implantation without pre-amorphization is not achievable with B implantation, since it requires a very high dose for amorphization. In addition, off-axis implantation is not effective in suppressing channeling at low B energy.[1] Even though Ga has a relatively low equilibrium solid solubility in Si, it can be implanted to high doses and does not precipitate upon rapid anneal ($\simeq$30 s) at low temperature ($\sim$600 °C). This is a critical feature since it allows for low thermal budget processing and hence minimizes the diffusion effects of Ga in the Si, as well as of Ga in any $SiO_2$ layers. In this paper we report on the fabrication of ultrashallow $p^+$–$n$ junctions using low energy Ga focused ion beam (FIB) implantation. The FIB implantation approach has the additional advantage of introducing Ga only in the Si region required for *p–n* junction fabrication. Therefore, during eventual *p*-channel MOSFET fabrication using Ga source and drain FIB implantation, no Ga would be introduced into the gate oxide.

## II. EXPERIMENTAL CONDITIONS

The substrates used for the experiments to be described here were ⟨100⟩-oriented 3-in. Si wafers, P-doped with a background concentration of $2\times10^{15}$ $cm^{-3}$. The wafers were RCA cleaned and subsequently a 200-nm-dry $SiO_2$ layer was thermally grown. The oxide layer was subsequently patterned to provide easy-to-recognize implanted regions. The $Ga^+$ implants were performed using a NanoFab 150 system manufactured by Microbeam Inc.[11] The NanoFab

 © 1990 American Vacuum Society 

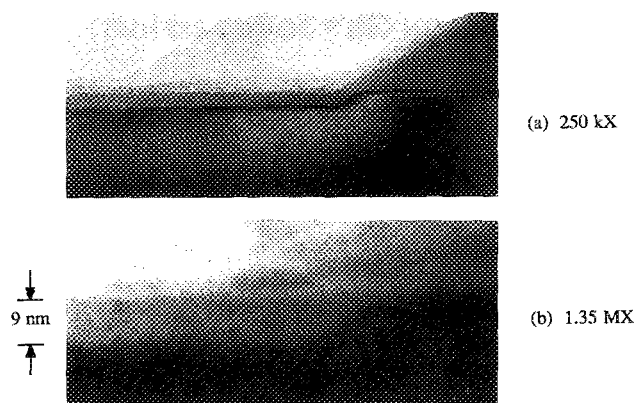


FIG. 1. Cross-section TEM photographs of 5-keV Ga As-implanted samples. (a) 250 kX magnification, (b) 1.35 MX magnification.

150 uses a two lens optical system in conjunction with an E×B mass filter ($M/\Delta M = 50$). The system pressure is in the $1\times10^{-7}$ Torr range. All NanoFab 150 parameters are controlled by an IBM PC/AT and imbedded microprocessors. The accelerating voltage can be varied from 4 to 150 keV, which varies the minimum beam step size from 304 to 8.1 nm. The beam diameter is adjusted to a value several times the minimum step size at each energy to ensure the spatial uniformity of the implant. The stage position is monitored with a laser interferometer and the computer software automatically compensates for differences in the mechanical and requested positions of the stage by introducing an appropriate deflection of the beam. The stage can hold substrates up to 7×7 in.$^2$ and small area implants can be performed at angles from 3° to 30°. A localized gas delivery system and secondary ion mass spectroscopy (SIMS) analyzer ($M/\Delta M \sim 200$) are also part of the system.

For these experiments, the liquid metal ion source of the FIB was charged with pure gallium and measurements with the E×B filter show the ion beam to contain $^{69}Ga^+$ and $^{71}Ga^+$ in the ratio of 60/40. The Ga beam was found to contain predominantly the singly ionized monomer specie: 99.6% $Ga^+$, 0.35% $Ga_2^+$, 0.05% $Ga^{++}$. The experiments were performed with the E×B filter off, producing a natural distribution of isotopes. Areas of 540×540 $\mu m^2$ were implanted on-axis at Ga energies ranging from 5 to 15 keV. Since these samples required large area exposures the beam was operated at a high target current of 450 pA. Hence, the beam diameter was much larger than would normally be used in actual $p$-$n$ junction fabrication. The implants were performed with a single serpentine scan using rates ranging from 0.15 cm/s (at 5 keV) to 0.5 cm/s (at 15 keV) to obtain a dose of $1\times10^{15}$ cm$^{-2}$. Ga FIB implant profiles have been shown[12] to be independent of scan rate in the 0.1 to 10 cm/s range. After FIB implantation, all wafers were heat treated by rapid thermal annealing using an AET-ADDAX RV system at 600 °C for 30 s in a $N_2$ ambient to recrystallize the material and to remove the damage caused by ion implantation. The ramp-up and ramp-down rates for the annealing cycle were both 40 °C/s.

## III. EXPERIMENTAL RESULTS

In this paper, we concentrate on the materials characterization of FIB implanted ultrashallow junctions. The analytical techniques used in this investigation include secondary ion mass spectroscopy (SIMS), spreading resistance profiling (SRP) and cross-sectional transmission electron microscopy (xTEM). These techniques impart essential information regarding the atomic and carrier concentration, junction depth, and implantation damage. While detailed electrical diode characteristics will be published elsewhere, preliminary current-voltage characteristics have been measured.

Transmission electron microscopy of cross-sectional samples offers an attractive means to study the damage due to implantation and the defects left behind after a heat treatment step to recrystallize the material. The procedure followed in this work for sample preparation is described elsewhere.[13] The TEM samples were analyzed using a Hitachi H600 and a Philips CM20 scanning transmission electron microscope. Figure 1 shows xTEM photographs of a 5-keV FIB $Ga^+$ implanted Si sample. In the right-hand side of the upper photograph the edge of the oxide layer is observed to coincide with the end of the amorphized Si region. The amorphized layer thickness, $t_A$, obtained from the lower

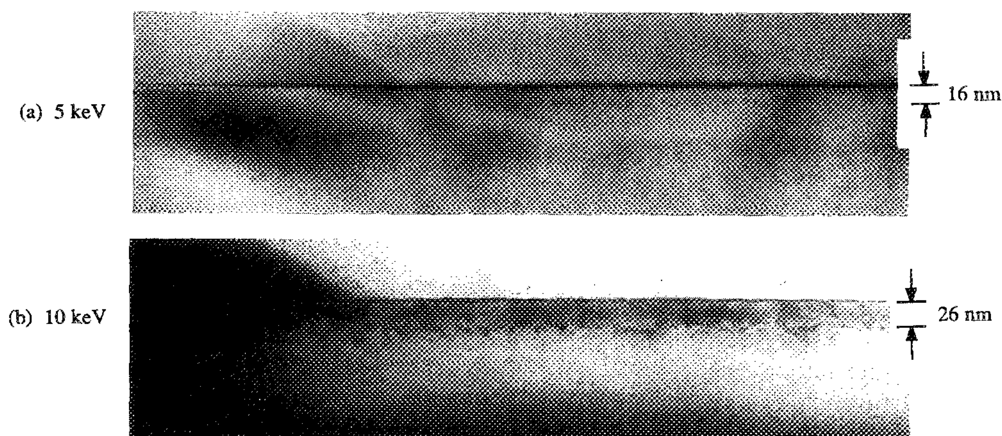


FIG. 2. Cross-section TEM photographs of annealed Ga implanted samples. (a) 5 keV, (b) 10 keV.

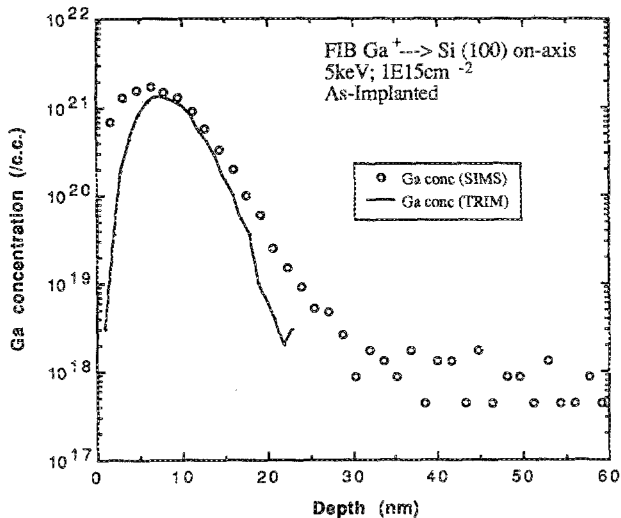


FIG. 3. SIMS depth profile of 5-keV Ga FIB implanted sample.

photograph at higher magnification measures approximately 9 nm. Figure 2 shows xTEM photographs of the 5- and 10-keV Ga-implanted Si samples after they have been annealed. The photographs clearly indicate that the damaged regions have recrystallized and the samples exhibit a line of end-of-range defects at a distance, $t_{EOR}$, of 16 and 26 nm, respectively, from the surface of the Si substrate. No other defects extending beyond the end-of-range region were detected.

SIMS, with a cesium primary ion beam, was used to observe the atomic concentrations of gallium in silicon for the as-implanted and annealed cases. A Cameca IMS-3f SIMS instrument was used with an effective 1-kV $Cs^+$ beam at a 60° impact angle. These conditions have been shown[14] to be necessary to minimize the mixing caused by the primary ion beam and thus result in the accurate SIMS depth profiling of shallow junctions. The Ga atomic concentration from a 5-keV, $1\times10^{15}$ cm$^{-2}$ implant is shown in Fig. 3. The peak in Ga concentration occurs at a depth of approximately 6.4 nm. Taking into account the native oxide thickness of 1–2 nm this results in a peak depth close to the 8.1 nm predicted by TRIM[15] for an amorphous sample. The major part of the depth profile exhibits a Gaussian dependence with only minor exponential decay into the substrate. The exponential tail can be due to a combination of effects, ion channeling during $Ga^+$ implantation and $Cs^+$ ion beam mixing during SIMS depth profiling. The scatter in data points around a value of $10^{18}$ cm$^{-3}$ at depths greater than 30 nm indicate the resolution limit of the SIMS instrument. Figure 4 shows the Ga depth profile resulting from the 15-keV FIB implantation. The peak in Ga concentration is at 16 nm, which is in excellent agreement with the TRIM value of 16.2 nm.

Spreading resistance profiling was performed on the $Ga^+$ implanted samples to obtain electrical characteristics. The SRP data for the 5-keV implant is shown in Fig. 5. The electrical $p^+$–$n$ junction occurs at a depth of $x_j \approx 20$ nm. Arrows indicate the edge of the pre-anneal amorphized region and the location of the end-of-range defects after recrystallization. It is interesting to note the approximate equality of $x_j$ and $t_{EOR}$. The junction depths measured for 10 and 15-keV $Ga^+$ implantation energies are 50 and 70 nm, respectively. SRP measurements of shallow junctions are subject to a number of effects which modify the results, including surface charge, effective mobility and carrier spilling.[16] Since an almost linear relationship between $x_j$ and implant energy was observed, it would appear that the junction depth values obtained are fairly accurate. The values of the carrier concentration in the $p^+$ region are probably a substantial underestimate since conventional $p$-type (i.e., B-doped) Si mobility is assumed, whereas Ga-doped Si is known to have a much smaller hole mobility.[17] Diodes have been fabricated using low energy $Ga^+$ FIB implantation. The $I$–$V$ charac-

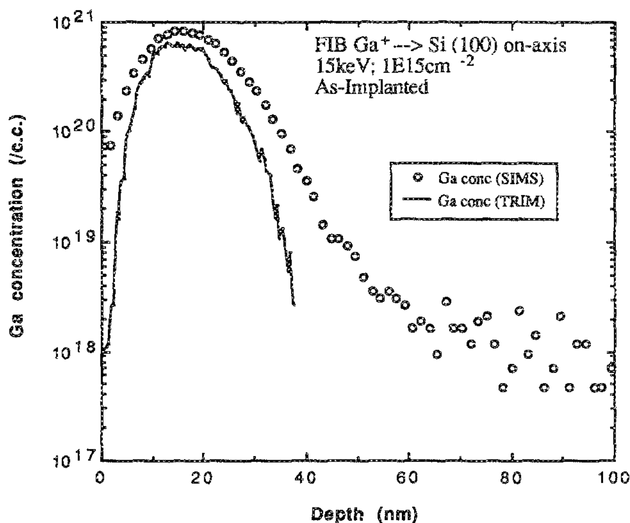


FIG. 4. SIMS depth profile of 15-keV Ga implanted sample.

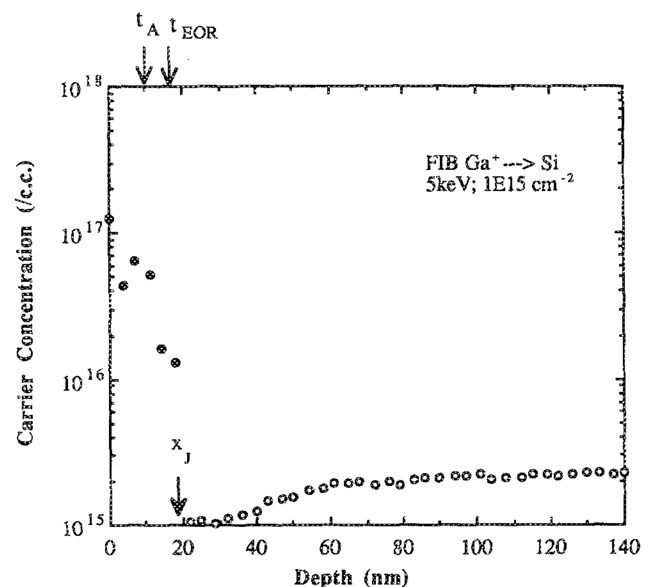


FIG. 5. Post-anneal SRP depth profile of 5-keV Ga FIB implanted $p^+$–$n$ junction.

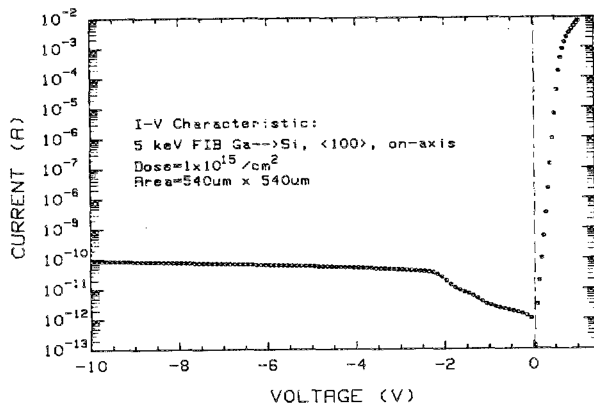


FIG. 6. Current-voltage characteristic of 5-keV Ga FIB implanted $p^+$–$n$ junction.

teristic of a 5-keV-implanted diode is shown in Fig. 6. The reverse bias current densities at 1, 5, and 10 V are 0.99, 20.4, and 31.62 nA/cm$^2$, respectively. The ideality factor for forward bias operation measured 1.059. These preliminary electrical results are quite encouraging, since they are comparable to leakage currents obtained in B-implanted diodes with substantially larger junction depth.[18]

## IV. CONCLUSIONS

Low energy Ga focused ion beam implants have resulted in ultrashallow $p^+$–$n$ junctions. Junction depths as shallow as 20 nm have been measured by SRP for 5-keV Ga$^+$ implantation. Experimental data obtained from xTEM indicate a fairly good agreement between the location of the end-of-range defect layer and the junction depth. While this junction depth is the shallowest reported to date, considerable work is still required to fully and accurately characterize all the relevant materials and electrical properties of these Ga$^+$ FIB implanted $p$–$n$ junctions.

## ACKNOWLEDGMENTS

The authors would like to acknowledge the assistance of A. K. Rai in the fabrication of TEM samples, of A. K. Rai and V. Vasudevan in the TEM analysis, of D. Griffis and J. Hunter for the SIMS analysis and useful discussions on the interpretation of SIMS data with J. Solomon. The SRP measurements were performed at Solecon Labs.

[1] S. N. Hong, G. A. Ruggles, J. J. Paulos, J. J. Wortman, and M. C. Ozturk, Appl. Phys. Lett. **53**, 1741 (1988).
[2] C. P. Wu, J. T. McGinn, and L. R. Hewitt, J. Electron. Mater. **18**, 721 (1989).
[3] G. A. Ruggles, S-N. Hong, J. J. Wortman, M. Ozturk, E. R. Myers, J. J. Hren, and R. B. Fair, Mater. Res. Soc. Proc. **128**, 611 (1989).
[4] C.-M. Lin, A. J. Steckl, and T. P. Chow, Appl. Phys. Lett. **52**, 2049 (1988).
[5] C.-M. Lin, A. J. Steckl, and T. P. Chow, Appl. Phys. Lett. **54**, 792 (1989).
[6] T. Kamins, *Polycrystalline Silicon for Integrated Circuit Applications* (Kluwer, Boston, 1988).
[7] L. Rubin, D. Hoffman, D. Ma, and N. Herbots, IEEE Trans. Electron. Devices **ED-37**, 183 (1990).
[8] T. Y. Hsieh, H. G. Chun, D. L. Kwong, and D. B. Spratt, Appl. Phys. Lett. **56**, 1778 (1990).
[9] C.-M. Lin, A. J. Steckl, and T. P. Chow, J. Vac. Sci. Technol. B **6**, 981 (1988).
[10] C.-M. Lin, A. J. Steckl, and T. P. Chow, IEEE Electron Device Lett. **EDL-9**, 597 (1988).
[11] N. W. Parker, W. P. Robinson, and J. M. Snyder, SPIE **632**, 76 (1986).
[12] C-M. Lin, Ph.D. dissertation, Rensselaer Polytechnic Institute, 1988.
[13] A. K. Rai, M. H. Rashid, P. P. Pronko, A. Ezis, and D. W. Langer, J. Electron Microsc. Technol. **5**, 50 (1987).
[14] J. L. Hunter, S. F. Corcoran, D. P. Griffis, and C. M. Osburn, J. Vac. Sci. Technol. A **8**, 2323 (1990).
[15] J. F. Ziegler, J. P. Biersack, and U. Littmark, *Stopping and Range of Ions in Matter* (Pergamon, New York, 1988), Vol. I.
[16] W. Vandervost and T. Clarysse, J. Electrochem. Soc. **137**, 679 (1990).
[17] M. Y. Tsai, B. G. Streetman, V. R. Deline, and C. A. Evans, J. Electron. Mater. **8**, 111 (1979).
[18] C. P. Wu, J. T. McGinn, and L. R. Hewitt, J. Electron. Mater. **18**, 721 (1989).